

Integrating and Live-time Radiation Dosimetry by Optical Crystal Damage, Initial Results with Neutrons

**Institute of Nuclear Materials Management
(INMM) Annual Meeting**

Adam Hecht, Jean-Claude Diels,
Ladan Arissian, Erin Vaughan
(University of New Mexico)

September 2015

The INL is a
U.S. Department of Energy
National Laboratory
operated by
Battelle Energy Alliance



This is a preprint of a paper intended for publication in a journal or proceedings. Since changes may be made before publication, this preprint should not be cited or reproduced without permission of the author. This document was prepared as an account of work sponsored by an agency of the United States Government. Neither the United States Government nor any agency thereof, or any of their employees, makes any warranty, expressed or implied, or assumes any legal liability or responsibility for any third party's use, or the results of such use, of any information, apparatus, product or process disclosed in this report, or represents that its use by such third party would not infringe privately owned rights. The views expressed in this paper are not necessarily those of the United States Government or the sponsoring agency.

Integrating and Live-time Radiation Dosimetry by Optical Crystal Damage, Initial Results with Neutrons

Adam Hecht, Jean-Claude Diels, Ladan Arissian, Erin Vaughan.*

University of New Mexico, Albuquerque, NM, USA.

** hecht@unm.edu*

Abstract

Radiation damage can be assessed through many techniques, though the assessment is usually offline and shows only integrated dose. Transparent crystals can be optically monitored for radiation damage nondestructively, to serve as a detector for both immediate dose and integrated dose for signatures of radiation exposure history. There is also some difference in gamma-ray and neutron interactions which can be observed. Gamma ray interactions primarily produce electron displacements, which are preserved as color centers in ionic crystals and produce specific spectral absorption lines. Neutron interactions strongly produce lattice displacements that affect the index of refraction. The differences may allow us to use inexpensive crystals for long time neutron monitoring. Spectroscopic absorption lines can be quantified using prior technology, but due to prior limits in phase sensitivity there was no previous use of index of refraction measurements. Using novel techniques based on intracavity phase interferometry to assess lattice displacements, we are able to examine neutron irradiation in CaF_2 crystals. Initial results with neutrons will be presented.

Introduction

Radiation damage to materials may be used to detect the presence or exposure to radioactive sources. Depending on the radiation field type (neutrons, electrons, gammas, etc.), dose rate and the presence of impurities, it is expected that certain materials may exhibit a characteristic response. By optically characterizing damage in transparent crystals we will characterize the radiation field.

By examining radiation damage to crystals we are effectively using an unpowered and inexpensive radiation detector that can be used for long term monitoring of radiation environments. By using nondestructive readout via optical methods, this enables both live-time and cumulative radiation dosimetry of the same sample.

It has been established that irradiation of ionic compounds by neutrons [1], gammas [2], electrons [3] and heavy ions [4] produces long term electron displacements and color centers, which can be observed in the crystal absorption spectrum. Previous work on radiation induced color centers in ionic crystals has largely been focused on the production of lasers for use in optical applications, and so the precise relation of gamma ray dose on color center production has yet to be thoroughly examined. We performed proof of concept experiments using CaF_2 , as it is a readily available, high purity, optically transparent ionic crystal. Different experiments were performed with gamma rays and with neutrons.

Gamma rays typically interact via electron interactions, with much of the energy going to electron recoils, which further ionize the atoms in the material. Different charge states of the atoms/molecules have different specific absorption lines, the color centers, and these electron displacements can be long lived in ionic crystals. For examining color centers we irradiated CaF_2 crystals with a ^{137}Cs source and compared transmission spectra versus unirradiated CaF_2 crystals.

While damage from gamma rays is dominated by electron displacements, neutrons, on the other hand, may cause considerable lattice displacements and damage [5] that are manifested by changes in the index of refraction. The extreme form this relation is the different indices of refraction of crystalline quartz and of amorphous quartz (fused silica), as presented in Figure 1. Bragg diffraction gratings along optical fibers have been used as index sensors to detect strain and temperature changes [6], but we are pushing here to low dose radiation. As photons primarily cause electron displacements rather than lattice displacements, we consider this a possible mode of developing gamma ray blind neutron detection. Note again, this is for a passive detection instrument that can be used for long term integrated dose or live time dosimetry only depending on when the optical readout is performed.

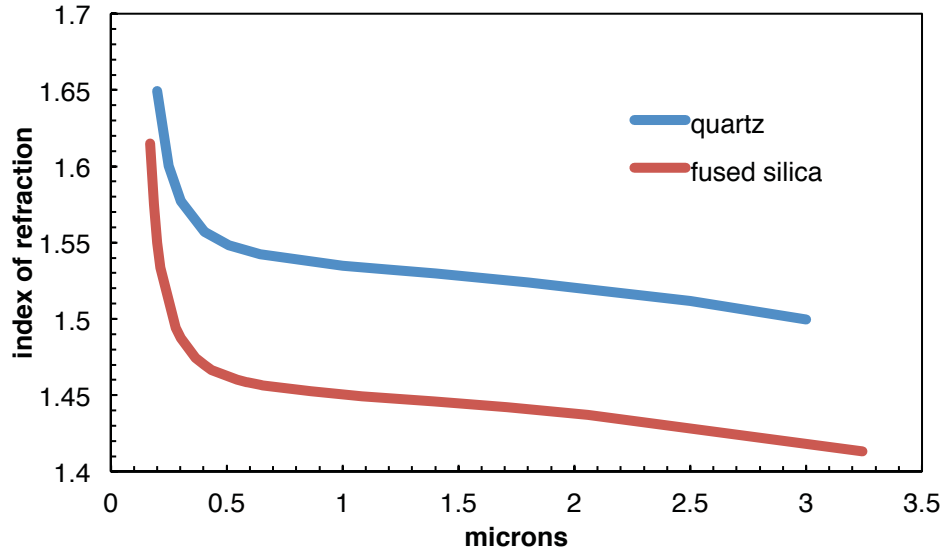


Figure 1. Indices of refraction vs. wavelength for crystalline quartz vs. amorphous fused silica.

We are introducing a new method of detecting changes of index with 10^{-7} resolution, a tremendous sensitivity to radiation effects. For proof of concept experiments on lattice displacements we introduce a new method of nested frequency combs with 10^{-7} resolution to examine a CaF_2 sample both before and after irradiation by a PuBe neutron source and have observed the index change. We expect to achieve a resolution of 10^{-10} by implementing a new method of intracavity phase interferometry [7].

Experiment - Color Centers

A CaF_2 crystal cylindrical disk of 25 mm diameter and 3 mm thickness was irradiated at room temperature using a 4.85×10^9 Bq ^{137}Cs source for increasing durations at 1.6×10^{-5} Gy/s. This is significantly less radiation than that reported by other researchers, which is on the order of 10^6 Gy for gammas, but we had the goal of determining lowest detectable limits and scaling in the linear response regime.

Spectra were measured using a Shimadzu UV1601PC Spectrophotometer. As a reference, a non-irradiated CaF_2 crystal was used to take differential measurements. Differential transmission spectrum results are shown in Figure 2 over a range of exposure times. The doses are proportional to the exposure times.

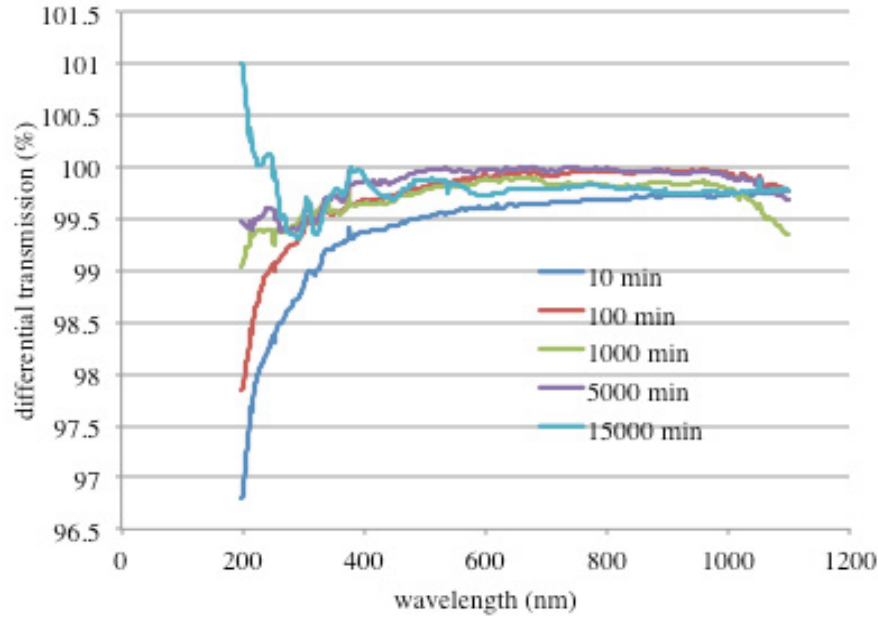


Figure 2. Differential measurement of transmission spectrum for CaF_2 exposed to a range of gamma ray doses divided by unirradiated CaF_2 .

There are several differences, with very significant difference at shorter wavelengths. The uncertainties, not given in the spectrometer readout, are certainly high near UV where transmission through air is strongly reduced. Experiments are being set up on a vacuum spectrometer to run further and with less uncertainty into the UV range. The increased intensity when UV strikes the sample may be due to increased fluorescence, as the photodiode is sensitive to a range of wavelengths. Discrimination of wavelengths leaving the sample must also be implemented.

Experiment - Index Change and nested frequency combs

We have developed a unique modelocked laser consisted of two nested combs, by insertion of a small Fabry-Perot etalon (FPE). In this configuration two radio frequencies are generated, a high frequency RF that is inversely proportional to the optical path (distance and index) in the Fabry-Perot etalon and a low RF inversely proportional to the optical path in the laser cavity. The sample to measure the index change is the Fabry-Perot etalon. By measuring the ratio between the high frequency and low frequency RF for irradiated and unirradiated Fabry-Perot, while tuning the laser cavity parameters such as cavity length or angle of the Fabry-Perot, we were able to determine the change of index between the two samples.

The parallel mirrors of a laser cavity give specific resonance modes, based on an integer number (m) of half wavelengths spanning the region between the mirrors (L), that is $m \lambda/2 = L$. There are an infinite number of longitudinal cavity modes, a picket fence pattern in frequency space. The gain medium emits photons over a small wavelength range from the relevant atomic transition, described by the transition width, and the overlap is a small range of the picket shaped resonances within the Lorentzian envelope. The cavity resonance, gain curve, and the resultant pulses are presented in frequency space in Figure 3.

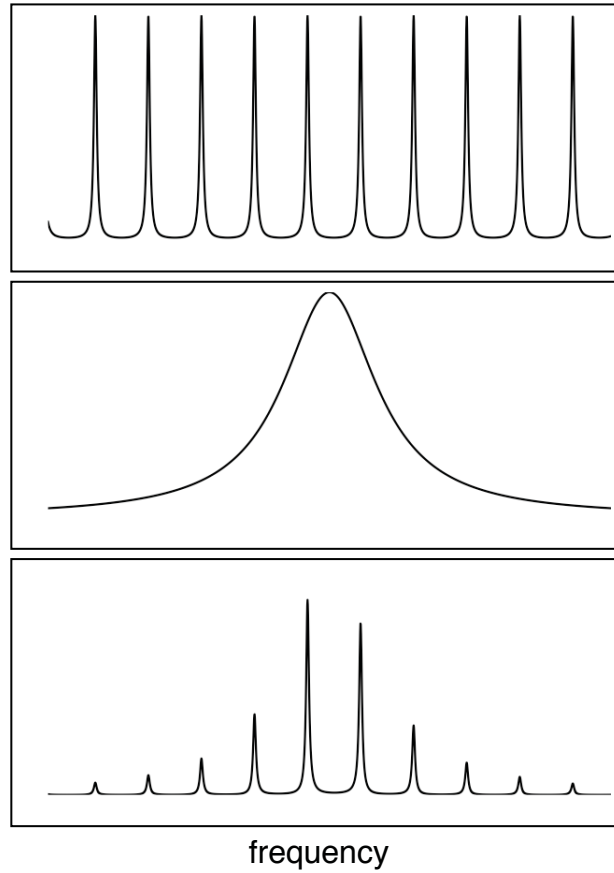


Figure 3. Schematic representation of a frequency comb, as from the Fabry-Perot etalon (top), the gain curve of the laser (middle), and the resultant frequency comb, as a function of frequency.

A solid crystal Fabry-Perot etalon is inserted into the laser cavity and has its own resonance conditions based on photon path length and index of refraction within the crystal. From a single light path entering, internal reflections produce interferences and the ratio of the transmitted to incident irradiance is the Airy function, $I_t/I_r = [1 + F \sin^2(\delta/2)]^{-1}$, where F is the coefficient of finesse. This function is dependent on the angle of the FPE to the incident light path, creating a picket fence pattern as a function of angle with maxima when the angle satisfies the Fabry-Perot resonance condition [8], when the phase is $\delta = (2m+1)\pi$ which can be expressed in terms of the FPE geometry as $[4\pi n/\lambda_0]d \cos \theta = (2m+1)\pi$.

The path lengths in the FPE are much shorter than for the full laser cavity, and the resonant wavelengths for the full cavity are much more closely spaced. That is, the cavity frequency comb is much tighter than the FPE frequency comb. The light must be at resonance for both the laser cavity and the FPE simultaneously, and can be represented by a product of the intensities as a function of frequency as in Figure 3. The resonance widths for the FPE follow the Airy function, with a low finesse (low reflectivity) FPE. The different combs are clear in Figure 4, representing the pulses in time, showing the wide time spaced repetition from the laser cavity and the narrow time spaced repetition from the FPE.

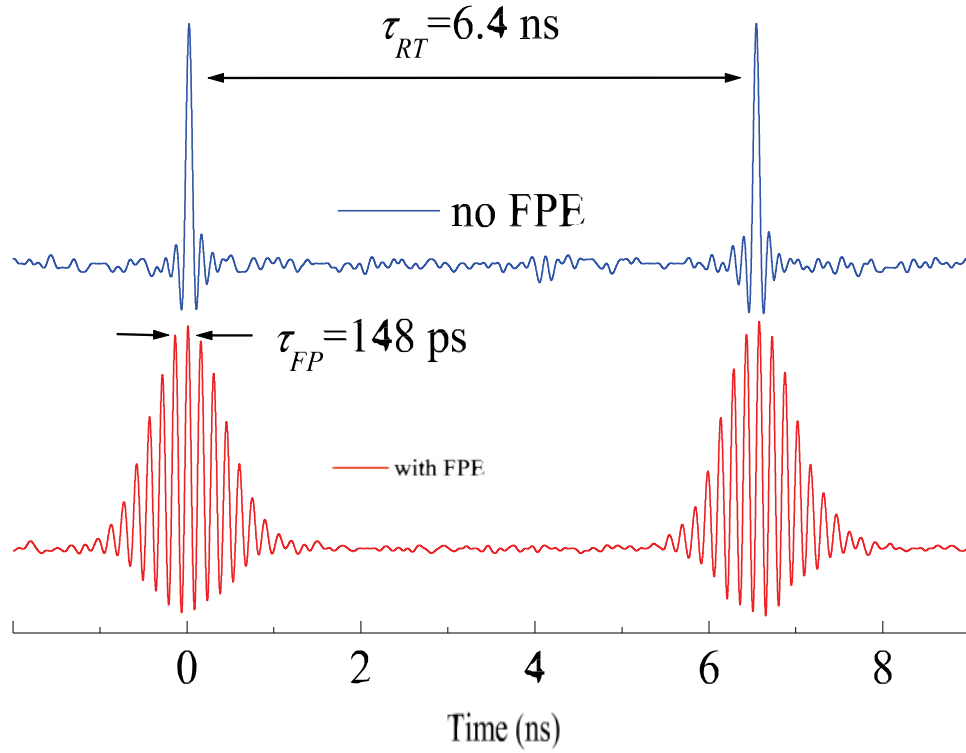


Figure 4. Time based schematic of the low repetition rate (large temporal spacing) from resonances with the full laser cavity length L (top) and the addition of a Fabry-Perot etalon with higher repetition rate (short temporal spacing) FPE resonances.

The light must be at resonance simultaneously with both the laser cavity and the crystal FPE, and be within the range of the lasing medium. The effective length of the cavity can be varied by slightly tilting the crystal FPE, and by changing the mirror position of the laser cavity, and creates different resonance conditions that can be examined, and the effective path length in the FPE is changed by tilting the crystal. The combination of the inserted FPE and the laser cavity produce surprising interactive effects.

Frequency representation may be described by the spacing between the high frequency components (HF) dominated by the laser cavity length L and index of refraction of the cavity, and by the spacing between the low frequency components (LF) dominated by the FPE thickness d and index of refraction. With a constant light wave the index of refraction refers to the velocity of the light phase. With pulses of light, the group velocity should be considered, which, in the laser, is dominated by gain and losses. The frequency ratio on resonance can be expressed in terms of the ratio of the group indices as

$$\frac{\nu_{FP}}{\nu_L} = \frac{n_{gL}}{n_{gFP}} \frac{L}{d}$$

where L is the laser cavity length, d the FPE thickness, and the subscripts L and FP refer to the laser cavity and the FPE. The phase indices are affected by the physical properties of the cavity but while the group index changes with the angle of the FPE the phase index does not. The L/d ratio can be expressed in terms of phase indices as

$$\frac{L}{d} = \frac{n_{pFP}}{n_{pL}} \frac{N_L}{N_{FP}}$$

thus, all other things considered, the ratio of the phase indices can be seen in the ratio of the HF and LF components of the resonant light pulse intensities,

$$\frac{\nu_{FP}}{\nu_L} = \frac{n_{gL}}{n_{gFP}} \frac{n_{pFP}}{n_{pL}} \frac{N_L}{N_{FP}}$$

where N_L and N_{FP} are integers for the different resonances. In this way, the ratios of the frequencies may be measured to give the ratio of the indices of refraction. By comparing crystals before and after irradiation, or comparing with an un-irradiated standard sample, very small radiation effects can be examined. The index change may be read out as the crystal is being damaged for a changing effect, or after integrating damage over time. Self annealing will be studied to this end.

Proof of concept measurements were performed on a CaF_2 crystal both before and after exposure to a 6 Ci PuBe neutron source for one day. A very small change of index of refraction was discernable using this technique, with the measurement being performed over a range of crystal angles and over a range of cavity lengths (mirror positions) to confirm measurement consistency and crystal angles (effectively changing the cavity length), see Figure 5. This is the first measurement of such a low change in the index of refraction, and the first measurement of such a low dose effect on lattice damage through index change.

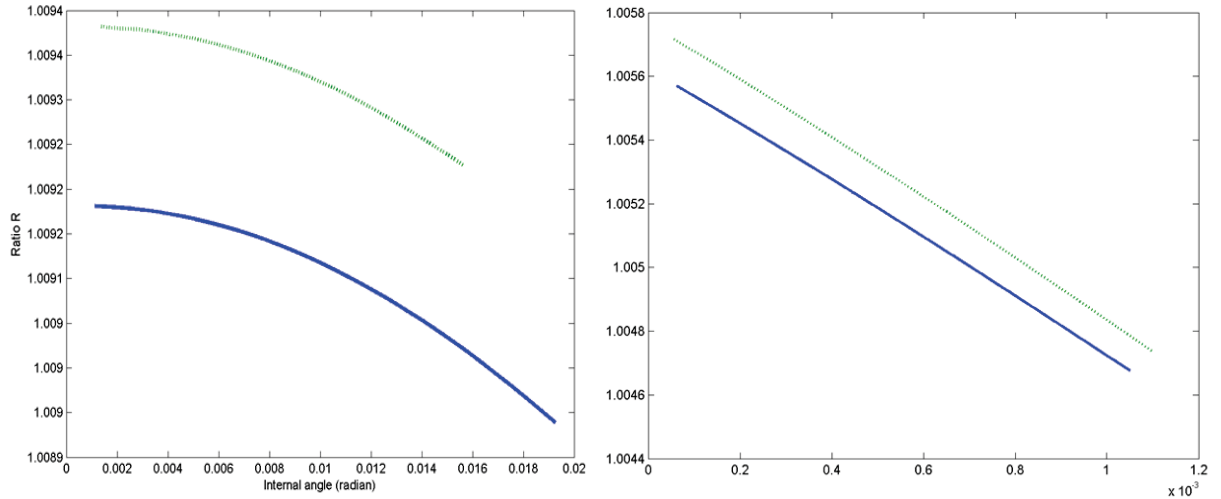


Figure 6. (a) Plot of ratio of high frequency to low frequency (HF/LF) normalized by the geometrical sizes tuning the angle of the Fabry-Perot etalon, changing the effective cavity length, and (b) directly tuning the cavity length by moving the end mirror. The top line in each figure is the pre-irradiated sample, the bottom is the same sample post neutron irradiation.

Acknowledgements

The authors acknowledge the dissertation work of Koji Masuda (PhD UNM 2014), under coauthor Diels, which contributed to this work.

References

1. T. Kamikawa, K. Ozawa, J. Phys. Soc. Japan 24 (1968).
2. V.V. Fedorov et al., Laser Phys. 1, 163 (2004).
3. T. Tsuboi, H.E. Gu, Applied Optics 33 (1994).
4. A. Rusakova et al., IOP Conf. Series: Materials Science and Eng. 38 (2012)
5. D. Olander, *Fundamental aspects of nuclear reactor fuels*, Technical Information Center, Office of Public Affairs, Energy Research and Development Administration, 1976.
6. W.W. Morey et al. Proc. SPIE 1169, Fiber Optic and Laser Sensors VII, 98 (1990).
7. L. Arissian and J.-C. Diels, Laser and Photonics Reviews - DOI 10.1002/lpor201300179 (2014).
8. E. Hecht, *Optics*, 4th ed., Addison Wesley, New York, 2001.